Biol. Cybern. 66, 19–25 (1991)

Biological Cybernetics

Noise effects on spike propagation in the stochastic Hodgkin–Huxley models

Y. Horikawa

Information and Computer Science Laboratory, Faculty of Education, Kagawa University, 1-1 Saiwai-cho Takamatsu, 760 Japan

Received September 21, 1990/Accepted in revised form July 12, 1991

Abstract. Effects of membrane current noise on spike propagation along a nerve fiber are studied. Additive current noise and channel noise are considered by using stochastic versions of the Hodgkin–Huxley model. The results of computer simulation show that the membrane noise causes considerable variation of the propagation time of a spike (thus changes in interspike intervals) for a small unmyelinated fiber of radius $0.1 \sim 1$ μm.

1 Introduction

Current and voltage fluctuation in nerve membrane can play an important role in neuronal information processing (Holden 1976; Tuckwell 1989). The studies of the stochastic models based on the space-clamped Hodgkin–Huxley model have shown that the membrane noise affects the probability of spike generation (Lecar and Nossal 1971; Skaugen and Walløe 1979), for instance.

In this paper, the effects of the membrane current noise on spike propagation along a nerve fiber (an axon) are studied on the basis of the Hodgkin–Huxley cable model. It is thought that a nerve fiber is a faithful transmission line of spikes. In the presence of the noise, however, a spike can generate on a fiber and can be extinguished during propagation, as shown in the space-clamped model. These phenomena are of interest, but are not studied here; because they would be treated as a spike generation problem including spatial form of a neuron (Skaugen 1980).

Here we study the case where a spike propagates on a fiber without failure, yet its speed is randomly varied owing to the noise during propagation, which is a problem inherent to a nerve fiber. Owing to the variation of the propagation speed, the propagation time of a spike from one end to the other on a fiber is randomly distributed, and interspike intervals of a spike train after propagation become different from those before propagation. These changes are important in nervous systems where the precise timing of occurrence of spikes or interspike intervals may carry information.

This paper is organized as follows. Expressions for the mean and variance of the propagation time are derived through a kinematic equation describing spike propagation in Sect. 2. In the following two sections, the results of computer simulation on stochastic versions of the Hodgkin–Huxley model are shown. In Sect. 3, Tuckwell's model is studied, in which the term of white noise in current is added to the Hodgkin–Huxley equations. As a more actual current noise source, in Sect. 4, Skaugen's model is studied, in which channel noise, i.e. random opening and closing of ion channels are considered. Spontaneous generation of spikes, changes in interspike intervals and relation to physiological knowledge are discussed in Sect. 5.

2 Kinematic description of spike propagation

The propagation speed of a spike on a nerve fiber can be determined by the state (principally the voltage) of fiber membrane ahead of a spike upstroke, which is based on the analyses of the experimental data of giant axons of the squid (Donati and Kunov 1976; Scott and Vota-Pinardi 1982) and is supported by the study of traveling solutions in the Hodgkin–Huxley model (Miller and Rinzel 1981). Thereby, when $t_0(x)$ denotes a time at which a spike upstroke is passing at a longitudinal position x of a fiber, its trajectory is described by

$$\mathrm{d}t_0(x)/\mathrm{d}x' = 1/\theta(V(x, t_0(x))$$
$$x' = x/\lambda \tag{1}$$

where $V(x, t_0)$ is the membrane voltage (which represents the membrane state) at the position of the spike upstroke and $\theta(V)$ is the propagation speed of the spike. We use here normalized length $x' = x/\lambda$, where λ is a space constant of membrane, so that $\theta(V)$ does not depend on a fiber radius, which we will use as a parameter in computer simulation in the following sections. A spike propagates at a constant speed $\theta(0)$ in

the resting state ($V(x, t_0) \equiv 0$) in the absence of the noise, i.e. propagation time $t_0(\lambda)$ per length λ is $1/\theta(0)$. When the voltage fluctuates by the membrane current noise, however, the speed is no longer constant during propagation.

When the fluctuation of $V(x, t_0)$ is small, $1/\theta(V)$ can be linearly approximated about $V = 0$. Thus (1) becomes

$$\mathrm{d}t_0(x)/\mathrm{d}x' = 1/\theta(0) + \beta V(x, t_0(x)) \tag{2}$$

where $\beta \simeq \mathrm{d}[1/\theta(0)]/\mathrm{d}V$, which is also independent of a fiber radius. We let the voltage fluctuation have zero mean ($E\{V(x, t_0)\} = 0$) without loss of generality.

We here approximate the membrane current noise as white noise in space and time. Note that $t_0(x)$ comes to the Wiener process in x, provided $V(x, t_0)$ is approximated by white noise. It is difficult, however, to derive the correlation of $V(x, t_0)$ because $V(x, t_0)$ is a function of the time $t_0(x)$, i.e. it depends on the trajectory of the spike. Thus we use a steady-state approximation based on the cable theory of passive membrane (MacGregor and Lewis 1977):

$$E\{V(x, t_0(x))V(y, t_0(y))\} = \sigma_\gamma^2 \exp(-|x-y|/\lambda)$$
$$\sigma_\gamma^2 = \sigma_I^2/(8\pi\alpha\lambda C g_m) \tag{3}$$

where σ_I^2 is an intensity of the current noise density, α is a fiber radius, λ is a space constant of membrane, C is membrane capacitance per unit area and g_m is membrane conductance per unit area. Here only the spatial correlation of the voltage is considered and the effects of its temporal correlation through $t_0(x)$ are neglected, since the expression for the spatial-temporal correlation is rather complicated (Tuckwell and Walsh 1983).

It follows that the mean $m(x)$ and variance $\sigma^2(x)$ of the propagation time $t_p(x)$ which it takes for a spike to propagate over length x are

$$m(x) = x/[\lambda\theta(0)] \tag{4}$$

$$\sigma^2(x) = \beta^2\sigma_\gamma^2[x/\lambda + \exp(-x/\lambda) - 1]\,. \tag{5}$$

The mean $m(x)$ is equal to a propagation time in the absence of the noise. Note that the means $m(\lambda) = 1/\theta(0)$ of the propagation times per space constant length are equal to one another for the arbitrary values of α, provided other membrane constants are fixed.

As for the variance $\sigma^2(x)$, we can approximate it by $\beta^2\sigma_\gamma^2 x/\lambda$ for $x \gg \lambda$. Hence the variance of the propagation time is about proportional to the propagation length, which corresponds to the Wiener process. For x fixed, e.g. for $x = \lambda$, the variance $\sigma^2(\lambda)$ per space constant length is proportional to the intensity σ_I^2 of the current noise density.

Furthermore, the fiber radius α affects the variation of the propagation time, i.e. $\sigma^2(\lambda)$ is proportional to $\alpha^{-3/2}$ since the space constant $\lambda \propto \alpha^{1/2}$. This is because σ_γ^2 is inversely proportional to the membrane area $S = 2\pi\alpha\lambda$ of length λ. Note that, when propagation length is measured with an absolute unit, e.g. x is in millimeters, the variance $\sigma^2(x)$ is proportional to x/α^2 and the standard deviation $\sigma(x)$ is proportional to $x^{1/2}/\alpha$. It is thus expected that the noise effects on the propagation time of a spike are considerable for a small (thin) fiber.

3 Additive white noise

Methods

We here consider the Hodgkin–Huxley model with additive current noise (Tuckwell 1989).

$$\begin{aligned}\alpha/(2R)\partial^2 V/\partial x^2 = {} & C\partial V/\partial t + \bar{g}_K n^4(V - V_K) \\ & + \bar{g}_{Na} m^3 h(V - V_{Na}) \\ & + g_L(V - V_L) + I(x, t)\end{aligned}$$
$$\partial n/\partial t = \alpha_n(1-n) - \beta_n n$$
$$\partial m/\partial t = \alpha_m(1-m) - \beta_m m$$
$$\partial h/\partial t = \alpha_h(1-h) - \beta_h h \tag{6}$$

and

$$\alpha_n = 0.01(10 - V)/\{\exp[(10 - V)/10] - 1\}$$
$$\beta_n = 0.125\exp(-V/80)$$
$$\alpha_m = 0.1(25 - V)/\{\exp[(25 - V)/10] - 1\}$$
$$\beta_m = 4\exp(-V/18)$$
$$\alpha_h = 0.07\exp(-V/20)$$
$$\beta_h = 1/\{\exp[(30 - V)/10] + 1\}\,. \tag{7}$$

The current noise density $I(x, t)$ is Gaussian white noise in space and time:

$$E\{I(x, t)\} = 0$$
$$E\{I(x, t)I(y, s)\} = \sigma_I^2/(2\pi\alpha)\delta(x - y)\delta(t - s)\,. \tag{8}$$

The intensity σ_I^2 of the current density is here taken to be 3.0×10^{-21} A^2/cm$^2 \cdot$ s, which is in the same order as the experimental data of the squid giant axon (Conti et al. 1975). We should note that the variation of the spike propagation depends on this value, i.e. $\sigma^2(x) \propto \sigma_I^2$ as has been derived in Sect. 2, when estimating the results in this section.

The values of membrane constants are (Hodgkin and Huxley 1952): $R = 35.4\ \Omega \cdot$ cm, $C = 1.0\ \mu$F/cm^2, $\bar{g}_{Na} = 120$ mS/cm^2, $\bar{g}_K = 36$ mS/cm^2, $g_L = 0.3$ mS/cm^2, $V_{Na} = 115$ mV, $V_K = -12$ mV and $V_L = 11$ mV. The fiber radius α is here treated as a parameter that determines the effects of the current noise. The space constant $\lambda = \{\alpha/[2R(\bar{g}_{Na}m^3(0)h(0) + \bar{g}_K n^4(0) + g_L)]\}^{1/2}$ is about $457\alpha^{1/2}$ μm and the membrane area $S = 2\pi\alpha\lambda$ of length λ is about $2871\alpha^{3/2}$ μm^2, where α is in micrometers. The values of α (corresponding λ and S) are taken to be as follows:

$\alpha = 0.1$ μm ($\lambda \simeq 0.14$ mm, $S \simeq 91$ μm^2);

$\alpha = 0.2$ μm ($\lambda \simeq 0.20$ mm, $S \simeq 257$ μm^2);

$\alpha = 0.4$ μm ($\lambda \simeq 0.28$ mm, $S \simeq 726$ μm^2).

Note that the lower bound of the radius of an actual unmyelinated fiber is about 0.1 μm. What we consider here is not the squid giant axon but a small (thin) fiber. The reason of using the above small values of α is that the variation of the propagation time is small compared with the time step Δt ($=2$ μs) used in the simulation even though $\alpha \simeq 1$ μm (see Results).

To numerically integrate (6), the explicit finite-difference method was used. A fiber was discretized into small segments of length $\Delta x = 0.2\lambda$ (a space step); the space step was taken to be relative to the space constant for each value of α. The equations were then integrated by the forward-Euler method with a time step $\Delta t = 2$ μs. The discretized equations were:

$$V(x, t+\Delta t) = V(x, t) + \{\alpha/(2R)[V(x+\Delta x, t) - 2V(x, t) + V(x-\Delta x, t)]/(\Delta x)^2 - \bar{g}_K n^4(x, t)[V(x, t) - V_K] - \bar{g}_{Na} m^3(x, t) h(x, t)[V(x, t) - V_{Na}] - g_L[V(x, t) - V_L] - I(x, t)\}\Delta t/C$$

$$I(x, t) = \sigma_I/(2\pi\alpha\Delta x\Delta t)^{1/2} W(x, t)$$

$W(x, t) \sim N(0; 1)$: the Gaussian distribution

$$n(x, t+\Delta t) = n(x, t) + \{\alpha_n[1 - n(x, t)] - \beta_n n(x, t)\}\Delta t$$

$$m(x, t+\Delta t) = m(x, t) + \{\alpha_m[1 - m(x, t)] - \beta_m m(x, t)\}\Delta t$$

$$h(x, t+\Delta t) = h(x, t) + \{\alpha_h[1 - h(x, t)] - \beta_h h(x, t)\}\Delta t$$

$$x = k\Delta x \qquad (k = 0, 1, 2, \ldots, L/\Delta x)$$

$$t = j\Delta t \qquad (j = 0, 1, 2, \ldots) \qquad (9)$$

Gaussian random variables $W(x, t)$ were generated using the Box–Muller method from uniform random numbers drawn from the VAX/FORTRAN random number generator. The values of Δx and Δt were chosen to be small enough to estimate the variation of the propagation time of a spike under the restrictions of computation time. It was verified that calculation with double the size of each step ($\Delta x = 0.4\lambda$ or $\Delta t = 4$ μs) had given about the same results on the mean and variance of the propagation time.

The total length L of the fiber was taken to be 11λ, which is considered to be actual length. A sealed-end boundary condition was assumed at both ends of the fiber. To generate a propagating spike, a current stimulus pulse (amplitude: 1.0 mA/cm^2, duration: 1.0 ms) was applied to one end ($x = 0$) of the fiber after 10 ms had passed in each run. The waiting time 10 ms was put in order that the membrane had then almost reached the stationary state. The time $t_0(x)$ at which the spike upstroke crossed the voltage 50 mV was recorded at each point of $x = 0, \lambda, 2\lambda, \ldots, 10\lambda$. The propagation time $t_p(x)$ over length x was then obtained by $t_0(x) - t_0(0)$.

For each value of α, there were 1000 runs made. Computation was done with VAX/FORTRAN on MICRO/VAX II.

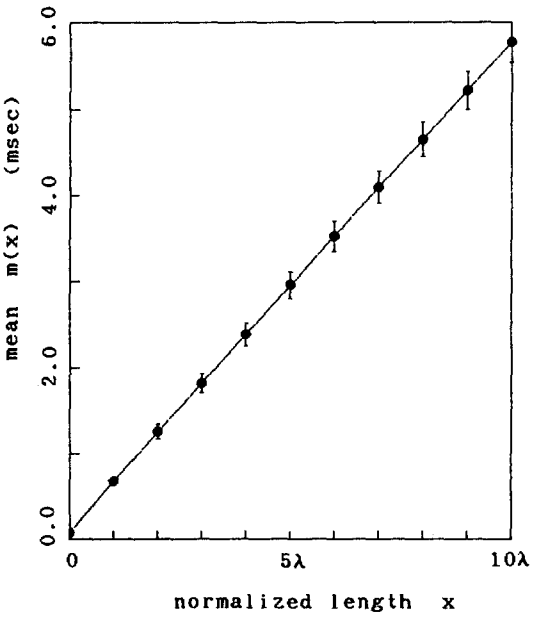

Fig. 1. The mean $m(x)$ of the spike propagation time vs. the propagation length x in the white noise model. The fiber radius is 0.1 μm (*closed circles*). Vertical markers denote 3σ-regions. The trajectory of a spike in the absence of the noise is plotted by a solid line

Results

Figure 1 shows the mean $m(x)$ of the spike propagation time $t_p(x)$ against the propagation length x. Only results for $\alpha = 0.1$ μm (closed circles) are plotted since the values of $m(x)$ for different three radii are almost equal to one another and are indistinguishable even though plotted. A solid line, which is almost straight, is the trajectory of a spike in the absence of the noise. It well agrees with $m(x)$; thus (4) proves to be a good approximation.

Figure 2 shows the variances $\sigma^2(x)$ of the propagation times for the different three radii. The simulation results are plotted by closed circles ($\alpha = 0.1$ μm), open circles ($\alpha = 0.2$ μm) and crosses ($\alpha = 0.4$ μm). They are well approximated by (5) (solid lines), in which the values of $\beta\sigma_\gamma^2$ are taken so that $\sigma^2(10\lambda)$ are equal to the values of the simulation results. The variances $\sigma^2(x)$ grow in nearly proportional to x for $x \gtrsim \lambda$.

The variances $\sigma^2(10\lambda)$ of the propagation time at $x = 10\lambda$ and corresponding standard deviations $\sigma(10\lambda)$ are:

$\sigma^2(10\lambda) = 6.26 \times 10^3$ μs^2, $\sigma(10\lambda) = 79$ μs, for $\alpha = 0.1$ μm ($10\lambda \simeq 1.4$ mm);

$\sigma^2(10\lambda) = 2.06 \times 10^3$ μs^2, $\sigma(10\lambda) = 45$ μs, for $\alpha = 0.2$ μm ($10\lambda \simeq 2.0$ mm);

$\sigma^2(10\lambda) = 0.66 \times 10^3$ μs^2, $\sigma(10\lambda) = 26$ μs, for $\alpha = 0.4$ μm ($10\lambda \simeq 2.8$ mm).

The ratios of $\sigma^2(10\lambda)$ are: $(6.26 \times 10^3)/(2.06 \times 10^3) \simeq 3.0$ and $(2.06 \times 10^3)/(0.66 \times 10^3) \simeq 3.1$, while both of the corresponding ratios of $\alpha^{-3/2}$ are $2^{3/2} \simeq 2.83$.

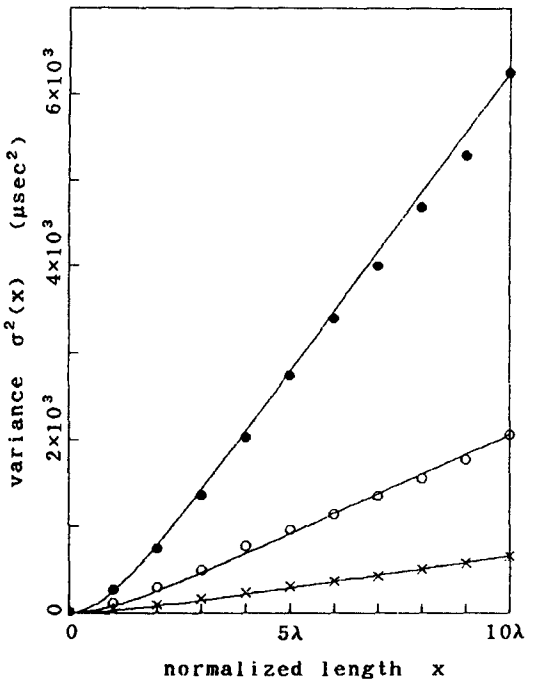

Fig. 2. The variance $\sigma^2(x)$ of the propagation time vs. the propagation length x in the white noise model. The fiber radii are 0.1 μm (*closed circles*), 0.2 μm (*open circles*) and 0.4 μm (*crosses*). The approximation by (5) is plotted by a solid line for each case

Both ratios of $\sigma^2(10\lambda)$ are slightly larger than the ratio of $\alpha^{-3/2}$, but are about equal to it. This agrees with the expression derived in Sect. 2 that $\sigma^2(x/\lambda)$ is proportional to $\alpha^{-3/2}$.

Vertical markers with closed circles in Fig. 1 denote the 3σ-regions of the propagation time for $\alpha = 0.1$ μm. The current noise can cause the considerable changes in spike trajectories for a fiber of radius in the order of 0.1 μm. The variation of the propagation time is smaller for larger fibers, however, since $\sigma(x/\lambda) \propto \alpha^{-3/4}$. When the fiber radius is 1 μm, for instance, $\sigma(10\lambda)$ is estimated to be smaller than 10 μs. Moreover, it is difficult to measure the variation for the squid giant axon of radius several hundred micrometers, in which $\sigma(10\lambda)$ ($10\lambda \simeq 10$ cm) is in the order of 0.1 μs.

4 Channel noise

Methods

We here consider random opening and closing of Na^+ and K^+ channels as a current noise source. We take Skaugen's model (Skaugen and Walløe 1979; Skaugen 1980) by slightly modifying to examine spike propagation:

$$\alpha/(2R)[V(x+\Delta x, t) - 2V(x,t) + V(x-\Delta x, t)]/(\Delta x)^2 = C\partial V(x,t)/\partial t + g_{Na}(x,t)[V(x,t) - V_{Na}] + g_K(x,t)[V(x,t) - V_K] + g_L[V(x,t) - V_L]$$

$$g_{Na}(x,t) = \bar{g}_{Na} n_{Na}(x,t)/N_{Na}$$

$$g_K(x,t) = \bar{g}_K n_K(x,t)/N_K \qquad (10)$$

where a fiber is discretized into the segments of length $\Delta x = 0.2\lambda$ (the space step) as in (9) in Sect. 3. Then N_{Na} and N_K denote the numbers of Na^+ and K^+ channels in one segment, while $n_{Na}(x,t)$ and $n_K(x,t)$ denote the numbers of *open* Na^+ and K^+ channels in each segment.

Each channel and each gate are assumed to act independently. The value of α's and β's calculated through (7) are used as the transition probabilities of opening and closing of corresponding gates. That is, the probability that a closed n-gate (m-gate, h-gate) will open in an interval Δt is $\alpha_n \Delta t$ ($\alpha_m \Delta t$, $\alpha_h \Delta t$); the probability that an open n-gate (m-gate, h-gate) will close in Δt is $\beta_n \Delta t$ ($\beta_m \Delta t$, $\beta_h \Delta t$). Moreover, to reduce computation time, the numbers of channels in closed states are here approximated by their mean values, which are expressed in terms of n, m and h calculated through the second, third and fourth equations in (6).

Under the above assumption and approximation, to obtain $n_{Na}(x,t)$ and $n_K(x,t)$, it suffices that we consider only the following six probabilities $\Pr\{S \to S'\}$ that a channel jumps from a state S to another S' in Δt and three numbers $N\{S\}$ of channels in a state S.

$$\Pr\{SN_{12} \to SN_{13}\} = \alpha_m \Delta t$$

$$\Pr\{SN_{03} \to SN_{13}\} = \alpha_h \Delta t$$

$$\Pr\{SN_{13} \to SN_{12}\} = 3\beta_m \Delta t$$

$$\Pr\{SN_{13} \to SN_{03}\} = \beta_h \Delta t$$

$$\Pr\{SK_3 \to SK_4\} = \alpha_n \Delta t$$

$$\Pr\{SK_4 \to SK_3\} = 4\beta_n \Delta t$$

$$\mathrm{N}\{SN_{12}\} = 3m^2(1-m)hN_{Na}$$

$$\mathrm{N}\{SN_{03}\} = m^3(1-h)N_{Na}$$

$$\mathrm{N}\{SK_3\} = 4n^3(1-n)N_K \qquad (11)$$

where SN_{kj} denotes the state of the Na^+ channel that k h-gates and j m-gates are open and SK_j denotes the state of the K^+ channel that j n-gates are open. The numbers of channels changing the state are given by a binomial distribution $\mathrm{Bin}(N;p)$; hence,

$$n_{Na}(x, t+\Delta t) = n_{Na}(x,t) + n_1(x,t) + n_2(x,t) - n_3(x,t) - n_4(x,t)$$

$$n_1(x,t) \sim \mathrm{Bin}(3m^2(1-m)hN_{Na};\ \alpha_m \Delta t)$$

$$n_2(x,t) \sim \mathrm{Bin}(m^3(1-h)N_{Na};\ \alpha_h \Delta t)$$

$$n_3(x,t) \sim \mathrm{Bin}(n_{Na};\ 3\beta_m \Delta t)$$

$$n_4(x,t) \sim \mathrm{Bin}(n_{Na};\ \beta_h \Delta t)$$

$$n_k(x, t+\Delta t) = n_K(x,t) + n_5(x,t) - n_6(x,t)$$

$$n_5(x,t) \sim \mathrm{Bin}(4n^3(1-n)N_K;\ \alpha_n \Delta t)$$

$$n_6(x,t) \sim \mathrm{Bin}(n_K;\ 4\beta_n \Delta t)\,. \qquad (12)$$

The single channel conductances γ_{Na} of the Na^+ channel and γ_K of the K^+ channel are taken to be 4 pS and 12 pS respectively, on the basis of the experimental data of the squid giant axon (Conti et al. 1975). The densities M_{Na} of the Na^+ channel and M_K of the K^+ channel are thus 300 μm^{-2} and 30 μm^{-2} respectively, in order that the maximum channel conductances $\bar{g}_{Na}$ and $\bar{g}_K$ agree with the values in the Hodgkin–Huxley model (120 mS/cm^2 and 36 mS/cm^2 respectively).

The computation method was same as described in Sect. 3. Equation (10) was integrated by the forward-Euler method with $n_{Na}(x, t)$ and $n_K(x, t)$ in (12). Binomial random variables $n_j(x, t)$ ($j = 1, 2, \ldots, 6$) in (12) were generated using the inverse function method from uniform random numbers. Values same as in Sect. 3 were taken as the space and time steps and the fiber radii ($\Delta x = 0.2\lambda$, $\Delta t = 2$ μsec and $\alpha = 0.1, 0.2, 0.4$ μm). The membrane area of one segment was $0.2S \simeq 574\alpha^{3/2}$ since $\Delta x = 0.2\lambda$. The channel numbers $N_{Na}(=0.2SM_{Na})$ and $N_K(=0.2SM_K)$ in one segment were:

$N_{Na} \simeq 5.4 \times 10^3$, $N_K \simeq 5.4 \times 10^2$, for $\alpha = 0.1$ μm;

$N_{Na} \simeq 1.5 \times 10^4$, $N_K \simeq 1.5 \times 10^3$, for $\alpha = 0.2$ μm;

$N_{Na} \simeq 4.4 \times 10^5$, $N_K \simeq 4.4 \times 10^4$, for $\alpha = 0.4$ μm.

Furthermore, to see which channel contributes to the variation of the propagation time, simulation was also made in the case where the proportion $n_{Na}(x, t)/N_{Na}$ of the number of open Na^+ channels was set equal to the mean value $m^3(x, t)h(x, t)$ and in the case where $n_K(x, t)/N_K$ was set equal to $n^4(x, t)$, both for $\alpha = 0.1$ μm.

Results

The means $m(x)$ of the propagation times for different three radii were almost equal to one another and agreed with the trajectory in the absence of the noise, as in Sect. 3; thus they are not presented here.

Figure 3 shows the variances $\sigma^2(x)$ of the propagation times (closed circles for $\alpha = 0.1$ μm, open circles for $\alpha = 0.2$ μm and crosses for $\alpha = 0.4$ μm). The simulation results are well approximated by (5) (solid lines), as in the case of white noise in Sect. 3, although the channel noise here has temporal correlation. The values of $\sigma^2(x)$ take the same order as those in Sect. 3. The values of $\sigma^2(10\lambda)$ and $\sigma(10\lambda)$ are:

$\sigma^2(10\lambda) = 4.33 \times 10^3$ μs^2, $\sigma(10\lambda) = 66$ μs, for $\alpha = 0.1$ μm;

$\sigma^2(10\lambda) = 1.50 \times 10^3$ μs^2, $\sigma(10\lambda) = 39$ μs, for $\alpha = 0.2$ μm;

$\sigma^2(10\lambda) = 0.55 \times 10^3$ μs^2, $\sigma(10\lambda) = 23$ μs, for $\alpha = 0.4$ μm.

The ratios of $\sigma^2(10\lambda)$ are: $(4.33 \times 10^3)/(1.50 \times 10^3) \simeq 2.9$ and $(1.50 \times 10^3)/(0.55 \times 10^3) \simeq 2.7$, both which agree with the corresponding ratio ($\simeq 2.83$) of $\alpha^{-3/2}$, as in Sect. 3.

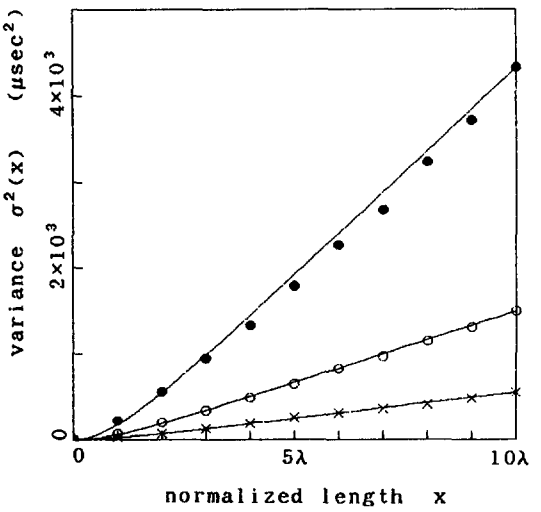

Fig. 3. The variance $\sigma^2(x)$ of the propagation time vs. the propagation length x in the channel noise model. The fiber radii are 0.1 μm (*closed circles*), 0.2 μm (*open circles*) and 0.4 μm (*crosses*). The approximation by (5) is plotted by a solid line for each case

Furthermore, Fig. 4 shows results in the case where the proportion of open Na^+ channels or open K^+ channels was set equal to the mean value of each. Closed circles denote the variance $\sigma^2_K(x)$ of the propagation time when only K^+ channels fluctuate, while open circles denote the variance $\sigma^2_{Na}(x)$ when only Na^+ channels fluctuate. We can see that the sum (a solid line) of $\sigma^2_K(x)$ and $\sigma^2_{Na}(x)$ about agrees with $\sigma^2(x)$ (crosses, same as closed circles in Fig. 3) in the case where both of Na^+ and K^+ channels fluctuate. Hence the Na^+ and K^+ channel noise may independently have effects on the membrane voltage and thus the propagation time.

The variance $\sigma^2_K(10\lambda)$ ($\simeq 3.8 \times 10^3$ μs) is about eight times as large as $\sigma^2_{Na}(10\lambda)$ ($\simeq 4.7 \times 10^2$ μs). However, the variances σ^2_{iNa} and σ^2_{iK} of current noise densities due to the Na^+ channel and the K^+ channel about the resting state ($V = 0$) are derived as (Stevens 1972):

$$\sigma^2_{iNa} = M_{Na}\gamma^2_{Na}m^3(0)h(0)(1 - m^3(0)h(0)) \simeq 6.3 \times 10^{-7}\ \mu A^2/cm^4;$$

$$\sigma^2_{iK} = M_K\gamma^2_K n^4(0)(1 - n^4(0)) \simeq 5.6 \times 10^{-7}\ \mu A^2/cm^4.$$

These two values are about equal, which disagrees with the above simulation results, provided the variance of the propagation time is proportional to the variance of the current density.

This disagreement may be attributed to the difference in temporal correlation between the Na^+ and K^+ channel noises. That is, the time constant of the n-gate of the K^+ channel at the resulting state in the Hodgkin–Huxley model is about 5.5 msec, while those of the m-gate and h-gate of the Na^+ channel are about 0.24 and 8.5 ms respectively. Hence, the current noise due to the K^+ channel may vary dozens of times as slowly as that due to the Na^+ channel, since the m-gates are dominant to opening and closing of the Na^+

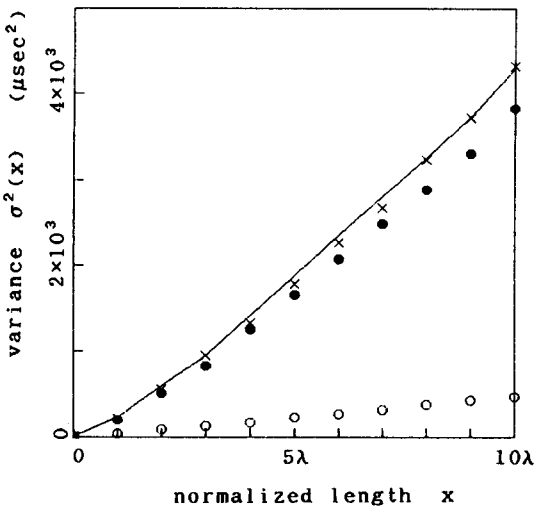

Fig. 4. The variance $\sigma^2(x)$ of the propagation time vs. the propagation length x in cases where only K^+ channels fluctuate (*closed circles*) and where only Na^+ channels fluctuate (*open circles*). The fiber radius is 0.1 μm. A solid line denotes the sum of the two values. Crosses denote the variance in the case where both kinds of channels fluctuate

channel about the resting state. Such a large time constant of the K^+ channel, which is about equal to the mean $m(10\lambda)$ of the propagation time over 10λ, may cause the variation of the propagation time larger than that expected from white noise with the same variance.

5 Discussion

Spontaneous generation and extinction of spikes

The membrane noise can cause the spontaneous generation of spikes in the cable model, although coupling by diffusion tends to suppress such a phenomenon. In fact, in simulation for $\alpha = 0.05$ μm, there occurred 154 times of spontaneous generations of spikes in the white noise model and 460 times in the channel noise model, before data of 1000 propagating spikes were obtained. (No extinctions of propagating spikes however occurred even in these case, which indicates the strength of the wave shaping action of a fiber.) The waiting time up to the addition of the stimulus pulse was 10 ms; hence the number of spikes spontaneously generating on a fiber of length $11\lambda \simeq 1.1$ mm reaches the order of $10^2\ s^{-1}$.

Consequently, an unmyelinated fiber is required to be larger than about 0.1 μm in radius in order to ensure transmission of spikes, provided the membrane properties are same as those of the squid giant axon. This value agrees with the lower bound in radius of actual unmyelinated fibers. Moreover, the variation of the propagation time proves to be bounded to the results obtained for $\alpha = 0.1$ μm ($\sigma(10\lambda) \simeq 10^2$ μs) on a fiber guaranteeing faithful transmission of spikes.

Changes in interspike intervals

We here consider a stationary spike train $(t_j(x);\ 0 \leqslant x \leqslant L,\ -\infty < j < \infty)$ propagating on a fiber. The propagation time $t_{pj}(x) = t_j(x) - t_j(0)$ of each spike is approximately independent when interspike intervals $T_j(x) = t_j(x) - t_{j-1}(x)$ are large compared with the refractory period of the fiber. A series of interspike intervals $\{T_j(x)\}$ thus gets negatively correlated during propagation, since $T_j(x)$ is a first difference for $t_{pj}(x)$. The power spectrum of $\{T_j(x)\}$ that was a regular spike train ($T_j(0) = \bar{T}$) at $x = 0$ is given by $2\sigma^2(x)[1 - \cos(\omega)]$, where $\sigma^2(x)$ is the variance of $t_p(x)$.

When the interspike intervals are small enough to lie in the refractory period, however, afterpotential of a spike affects the speed of the succeeding spike (Horikawa 1989). The expression for the correlation of $\{T_j(x)\}$ is thus more complicated owing to interaction between spikes. It can be shown, however, that $\{T_j(x)\}$ approaches a white noise series with a finite variance as x tends to ∞.

Relation to physiological knowledge

Measurement of spike speeds on actual small nerve fibers may already have estimated the variation of propagation time experimentally. The only experimental data that the author knows is, however, that on the frog sciatic nerve fiber (Lass and Abeles 1975). It has been shown that the standard deviation of the propagation time due to the noise is bounded to less than $3 \sim 5$ μs on the fibers of length 10 cm and of radius several μm. This value is smaller than that estimated from the results in this paper. The sciatic fiber is, however, myelinated. The noise effects on a myelinated fiber are expected to be smaller than those on an unmyelinated fiber, since membrane currents are passive in regions covered with myelin sheaths.

In the simulation, the Hodgkin–Huxley model was used as a standard model of a nerve fiber and simple assumptions were put on the membrane noise. Actual nerve fibers have various properties that we should take account of: differences in mechanisms of spike generation between the squid giant axon (the Hodgkin–Huxley cable model) and a small unmyelinated fiber, e.g. a sodium-potassium pump, ionic concentration in intracellular and extracellular regions, calcium-dependent potassium conductance and ionic diffusion (Scriven 1981; Qian and Sejnowski 1989); channel density and single channel conductance relative to the size of fibers (Jack 1975); intrachannel cooperativity and interchannel coupling (Holden 1982); spatial distribution of channels (Waxman and Ritchie 1985); intensity of the membrane noise and contribution of thermal noise and 1/f noise (Lecar and Nossal 1971; Stevens 1972). Moreover, most nerve fibers are non-uniform, branched and bundled together. The results in this paper, however, can present some quantitative estimates of the effects of the noise on spike propagation and show that the propagation time can vary in the order of 10^2 μsec on a small unmyelinated fiber of actual length.

The variation of the propagation time and changes in interspike intervals studied here are of little importance in most nervous systems, in which the spike

frequency code are used. In the central nervous system, however, there exist systems in which the precise timing of spikes is of importance. In an auditory system detecting interaural time differences on a microsecond time scale, it has been suggested that the axons of the nucleus magnocellularis neurons entering into the nucleus laminaris act as delay lines of spikes in an owl (Konishi et al. 1988) and in a chick (Young and Rubel 1983). Moreover, in the adaptive filter model of the cerebellum, parallel fibers (which are about 0.1 μm in radius and are a few millimeters in length) act as the transmission lines of signals from the granule cells to the Purkinje cells (Fujita 1982). The variation of the propagation time on the fibers due to the noise may bound sensitivity of these systems.

6 Conclusions

The variation of the propagation time of a spike along a nerve fiber due to the membrane current noise was studied. The kinematic description of spike propagation showed that the variance of the propagation time varies as the propagation length, and that the variance per space constant length varies inversely as the fiber radius to three-halves power.

The computer simulation was done for a small unmyelinated fiber by using the stochastic versions of the Hodgkin–Huxley model, in which the additive current noise and the channel noise were considered, on the basis of the experimental data of the squid giant axon. It was shown that the variation of the propagation time is considerable when a fiber radius is in the order of 0.1 μm. The standard deviation of the propagation time for a fiber of radius 0.1 μm and of length 1 mm reached 100 μs, for instance (in which case the mean of the propagation time was about 6 ms).

Furthermore, spikes often generated spontaneously on a fiber of radius 0.05 μm in the simulation. Thus, the order of 0.1 μm was given as the lower bound of the radius of an unmyelinated fiber, and the order of 10^2 μs was given as the upper bound of the standard deviation of the propagation time over actual length.

References

Conti F, De Felice LJ, Wanke E (1975) Potassium and sodium ion current noise in the membrane of the squid giant axon. J Physiol (London) 248:45–82

Donati F, Kunov H (1976) A model for studying velocity variations in unmyelinated axons. IEEE Trans Biomed Eng BME23:23–28

Fujita M (1982) Adaptive filter model of the cerebellum. Biol Cybern 45:195–206

Hodgkin AL, Huxley AF (1952) A quantitative description of membrane current and its application to conduction and excitation in nerve. J Physiol (London) 117:500–544

Holden AV (1976) Models of stochastic activity of neurons. Springer, New York Berlin Heidelberg

Holden AV (1982) Stochastic, quantal membrane conductances and neuronal function. In: Amari S, Arbib MA (eds) Competition and cooperation in neural nets. Springer, New York Berlin Heidelberg

Horikawa Y (1989) Filtering properties due to velocity dispersion on an axon (in Japanese). Trans IEICE Jpn 72-D-2:621–629

Jack JJB (1975) Physiology of peripheral nerve fibers in relation to their size. Br J Anaesth 47:173–182

Konishi M, Takahashi TT, Wagner H, Sullivan WE, Carr CE (1988) Neurophysiological and anatomical substrates of sound localization in the owl. In: Edelman GM, Gall WE, Cowan WM (eds) Auditory function. Wiley, New York, pp 721–745

Lass Y, Abeles M (1975) Transmission of information by the axon: I. noise and memory in the myelinated nerve fiber of the frog. Biol Cybern 19:61–67

Lecar H, Nossal R (1971) Theory of threshold fluctuations in nerves. Biophys J 11:1048–1084

MacGregor RJ, Lewis ER (1977) Neural modeling. Plenum Press, New York

Miller RM, Rinzel J (1981) The dependence of impulse propagation speed on firing frequency, dispersion, for the Hodgkin–Huxley model. Biophys J 34:227–259

Qian N, Sejnowski TJ (1989) An electro-diffusion model for computing membrane potentials and ionic concentrations in branching dendrites, spines and axons. Biol Cybern 62:1–15

Scott AC, Vota-Pinardi U (1982) Velocity variations on unmyelinated axons. J Theor Neurobiol 1:150–172

Scriven DRL (1981) Modelling repetitive firing and bursting in a small unmyelinated nerve fiber. Biophys J 35:715–730

Skaugen E (1980) Firing behaviour in nerve cell models with a two-state pore system. Acta Physiol Scand 109:377–392

Skaugen E, Walløe L (1979) Firing behaviour in a stochastic nerve membrane model based upon the Hodgkin–Huxley equations. Acta Physiol Scand 107:343–363

Stevens CF (1972) Inferences about membrane properties from electrical noise measurements. Biophys J 12:1028–1047

Tuckwell HC (1989) Stochastic processes in the neuroscience. SIAM, Philadelphia

Tuckwell HC, Walsh JB (1983) Random currents through nerve membranes. Biol Cybern 49:99–110

Waxman SG, Ritchie JM (1985) Organization of ion channels in the myelinated nerve fiber. Science 228:1502–1507

Young SR, Rubel EW (1983) Frequency-specific projections of individual neurons in chick brainstem auditory nuclei. J Neurosci 3:1373–1378

Yo Horikawa
Information and Computer Science Laboratory
Faculty of Education
Kagawa University
1-1 Saiwai-cho Takamatsu
760 Japan